Molecular pathology analyses of two fatal human infections of avian influenza A(H7N9) virus

Yanling Feng,[1] Lvyin Hu,[2] Shuihua Lu,[3] Qingguo Chen,[3] Ye Zheng,[1] Dong Zeng,[1] Jun Zhang,[2] Anli Zhang,[4] Liang Chen,[5] Yunwen Hu,[6] Zhiyong Zhang[7]

► Additional material is published online only. To view please visit the journal online (http://dx.doi.org/10.1136/jclinpath-2014-202441).

[1]Department of Pathology, Shanghai Public Health Clinical Center, Fudan University, Shanghai, China
[2]Department of Clinical Laboratory, Shanghai Public Health Clinical Center, Fudan University, Shanghai, China
[3]Department of Respiratory Medicine, Shanghai Public Health Clinical Center, Fudan University, Shanghai, China
[4]Scientific Research Center, Shanghai Public Health Clinical Center, Fudan University, Shanghai, China
[5]Department of Viral Hepatitis, Shanghai Public Health Clinical Center, Fudan University, Shanghai, China
[6]Department of Pathogen Diagnosis and Biosafety, Shanghai Public Health Clinical Center, Fudan University, Shanghai, China
[7]Department of Radiology, Shanghai Public Health Clinical Center, Fudan University, Shanghai, China

Correspondence to
Dr Yanling Feng, Shanghai Public Health Clinical Center, 2901 Caolang Road, Jinshan, Shanghai 201508, China; fengyanling@shaphc.org

YF, LH and SL contributed equally.

Received 29 May 2014
Revised 17 September 2014
Accepted 12 October 2014
Published Online First 6 November 2014

To cite: Feng Y, Hu L, Lu S, *et al. J Clin Pathol* 2015;**68**:57–63.

ABSTRACT

Aims To investigate the histopathological manifestations of two fatal cases of H7N9 influenza A virus infection.

Methods Pulmonary and hepatic specimens from two fatal cases of H7N9 influenza virus infection were examined using H&E staining. Additionally, in situ hybridisation was performed with probes (ViewRNA) targeting H7N9 RNA and IP-10, interleukin (IL)-6 mRNA. The distribution of surfactant protein A (SP-A), surfactant protein B (SP-B), CD3, CD4, CD8, CD68 and C4d were determined with immunohistochemistry.

Results Apart from the typical diffuse alveolar damage and hyaline membrane observed in severe influenza infection, we detected H7N9 RNA and massive intrapulmonary production of IP-10 and IL-6 mRNA using in situ hybridisation. Hyperplasia of type II pneumocytes was observed by H&E staining and immunohistochemistry. Proliferating macrophages and clustered neutrophils in the infected lungs were observed, whereas T lymphocytes, especially CD4T helper cells, were markedly depleted. No obvious complement deposition was found in lung tissues.

Conclusions Our findings suggest that H7N9 influenza virus induced an immunological response towards overt pulmonary inflammation and systemic lymphopenia which led to intense alveolar damage and respiratory failure.

INTRODUCTION

Human infections by a novel H7N9 avian influenza virus in eastern China were first reported on 30 March 2013.[1] The epidemic curve of the first wave of human infection spanned the period from mid-February to the end of May 2013, and comprised 132 human infections with a case fatality rate of 28%. Sporadic cases have been subsequently reported in the summer and fall of 2013. The second wave of human infections from the winter of 2013 to the spring of 2014 has resulted in over 200 confirmed cases.

Although extensive analyses have been made on clinical, immunological, radiological and epidemiological features of H7N9-infected individuals,[2–6] there are still limited in-depth reports describing the pathological manifestations of severe H7N9 infection.[7] Particularly, detection of viral and host transcripts in the infected tissue by a sensitive method of in situ hybridisation have not been described. To further characterise the immunopathogenesis of H7N9 influenza in humans, we performed a comprehensive analysis of lung and liver specimens from two patients who died of H7N9 influenza using H&E staining, immunohistochemistry and in situ hybridisation. We visualised the foci of viral replication and transcripts of inflammatory-response genes including IP-10 and interleukin (IL)-6. Analyses of markers for type II pneumocytes, macrophage, complement activation, T helper and cytotoxic T lymphocytes were further performed by immunohistochemistry.

MATERIAL AND METHODS

Patients

Patient No 1, (patient No 2 as per previous report[3]), male, aged 88 years, without history of contact with poultry and birds, but with a history of hypertension, diabetes mellitus, chronic bronchitis and coronary heart disease, started with an onset of fever, cough, expectoration with streaks of blood and flu-like symptoms on 10 April 2013. Laboratory results showed increased hepatic and cardiac-associated enzymes (gamma-glutamyl transpeptidase, lactic dehydrogenase), high counts of neutrophils and low counts of lymphocytes. Afterwards, his cough and expectoration was aggravated with chest tightness and tachypnoea, and on the sixth day after the onset, the pharynx swab tested positive for H7N9 RNA. X-ray showed scattered patchy shadows in the lungs, especially in the middle and lower fields of the right lung which further deteriorated into diffuse high-density shadows (see online supplementary figure 1A). The patient began to develop acute respiratory distress syndrome (ARDS) and cardiac failure on the eighth day of the onset, and died of multiple organ failure on the 19th day despite antiviral (Oseltamivir 150 mg twice daily and Peramivir 0.6 g once daily) therapy and extracorporeal membrane oxygenation.

Patient No 2, male, aged 87 years, with occasional contacts with wet market poultry, without major underlying disease, started with fever and tachypnoea on 4 April 2013. On day 6 after disease onset, his condition quickly deteriorated into respiratory failure with diffuse ground-glass opacities in his right lung and patchy opacities in his middle and lower fields of the left lung on chest radiograph. His laboratory results were similar to those of patient 1. His pharyngeal samples tested positive for H7N9 RNA on the same day. He was transferred to intensive care unit (ICU) and ventilated mechanically. Oseltamivir (75 mg twice daily, which was doubled afterwards) and antibiotics (piperacillin and tazobactam 4.5 g every 8 h) were administered. However, his condition did not improve and he presented with lowered consciousness. His late-stage X-ray image is shown in online supplementary figure 1B. He developed ARDS and died on the 17th day after disease onset.

Postmortem biopsies

Postmortem biopsies within 1–2 h after death were obtained from the right lung at the fifth to sixth intercostal space posteriorly and the liver (from patient 2) at the ninth intercostal space using Trucut 18G needle. All procedures were performed aseptically according to standard guidelines, and were approved by the ethics committee of Shanghai Public Health Clinical Center. Both patients' family members provided written informed consent to limited postmortem biopsy.

Histopathology

After postmortem biopsy, three blocks of pale and beige lung tissues, which were 1.8 cm, 1.5 cm, 1.2 cm in length and about 0.15–0.2 cm in diameter were obtained from patient 1. In patient 2, two blocks of lung tissues with 1.2 cm, 1.0 cm in length and 0.15–0.2 cm in diameter, two blocks of liver tissues with 1.5 cm, 0.8 cm in length and 0.15–0.2 cm in diameter were recovered. Pulmonary and hepatic specimens were fixed with 4% neutral formaldehyde for 20 h, routinely dehydrated and embedded; 4 μM sections were serially cut on APES (3-Aminopropyltriethoxysilane)-coated microscope slides and stained with H&E and observed under a light microscope.

In situ hybridisation

The ViewRNA technology (Affymetrix, California, USA) was used to detect the plus strand of H7N9 influenza nucleoprotein (NP) segment and IL-6 and IP-10 messenger RNA. All the probe sets were ordered from Affymetrix (human IL-6, IP-10 mRNA and H7N9 NP plus strand, reference sequence KC853225.1). The hybridisation and amplification procedures were performed using the QuantiGene ViewRNA ISH Tissue Assay kit (Affymetrix, California, USA) according to the protocols provided by the manufacturer with minor modifications. After pretreatment, hybridisation, and amplification, sections were finally stained with nitro blue tetrazolium and 5-Bromo-4-chloro-3-indolyl phosphate (Roche) in developing solution at 37°C and counterstained with nuclear fast red. Slides were dehydrated and mounted with Ultra-Clear (Baso, China). To confirm the specificity of the H7N9 probe set, lung tissues from H7N9-infected C57BL6 mice and histologically normal lung were hybridised in parallel as positive and negative controls, respectively. To detect IL-6 and IP-10 mRNA by in situ hybridisation, we used sections from a histologically normal lung as negative control.

Immunohistochemistry

For immunohistochemistry, sections were routinely dewaxed and rehydrated. After appropriate heat-induced antigen retrieval, sections were incubated with the primary monoclonal antibody against the surfactant protein A (SP-A) (clone 32E12, type II pneumocyte), surfactant protein B (SP-B) (clone SPB01, type II pneumocyte), CD3 (clone PS1, T lymphocyte), CD4 (clone 4B12, T helper cell), CD8 (clone C8/144B, cytotoxic T lymphocyte), CD68 (clone KP1, macrophage) or C4d (clone SP91, marker for complement activation), respectively. After washing, Envision rabbit antimouse peroxidase polymer conjugate (Dako) was incubated for 30 min at room temperature and developed with 3,3′-diaminobezdine. Sections were counterstained with Mayer's haematoxylin. A lung specimen with normal histomorphology was used as a control for SP-A, SP-B, CD3, CD4, CD8, C4d and CD68 immunohistochemistry. Lung sections of a patient infected with Aspergillus were used as a positive control for C4d activation.

RESULTS

The microscopic features of lung pathology in these two patients were generally similar, that is, diffuse alveolar injury, widened alveolar septum (figure 1A), type II pneumocyte hyperplasia (figure 1B, black arrows) and diminished alveolar spaces. In patient 1, who died 19 days after disease onset, red stained, homogeneous, hyaline membrane formed on alveolar wall was observed (figure 1C, green arrows). Additionally, inflammatory cell infiltration and exudation were prominent (figure 1C, black arrows) with neutrophils in domination and rare lymphocytes (figure 1D). The exudate organisation in alveolar space and local fibrosis together promoted the pulmonary consolidation as observed in the radiographs (see online supplementary figure 1A) and in figure 1E. In patient 2, who died 17 days after disease onset, he also had notable pulmonary fibroproliferative changes (figure 1F). Hyaline membrane was also observed. Additionally, coarse or fine strands of fibrin were present in it (figure 1F), indicative of fully developed, influenza virus-induced pneumonia.[8] Additionally, intra-alveolar haemorrhage (figure 1G) was also documented. The main findings in his liver sections were: light hydropic degeneration of a few liver cells, fatty degeneration in about 5% of hepatocytes and focal hepatocytes necrosis accompanied by phlogocyte infiltration (figure 1H, black arrows).

Using the oligonucleotide probe set targeting NP mRNA, we performed in situ hybridisation to visualise the site of viral replication. We detected low levels of H7N9 NP mRNA in the cytoplasm and nucleus of a few alveolar epithelial cells after prolonged staining in patient 1 (figure 2 A). As a positive control experiment, we employed lung specimens from experimentally infected C57BL/6 mice which exhibited an intense signal after 30 min of development (figure 2B). No NP mRNA was detected in the liver tissue of patient 2 (data not shown) and, as expected, no signal was obtained in a histologically normal lung tissue (figure 2C).

The typical inflammatory response as observed in H&E staining prompted us to investigate the expression of various inflammation mediators like IP-10 and IL-6. Using ViewRNA in situ hybridisation, we observed the highly elevated and widely distributed transcripts of IP-10 in the alveolar space and surrounding tissues (figure 2D). Additionally, expression of IL-6 mRNA was detected although weaker than IP-10 mRNA (figure 2F). By contrast, IP-10 and IL-6 mRNA were not induced in normal lung tissue (figure 2E, G). These results are in agreement with the observation that hypercytokinaemia in peripheral blood is typical of severe H7N9 infection.

Since type II pneumocytes are widely recognised as the pulmonary target cell for both H7N9 and H5N1 influenza virus,[9–11] we examined the status of SP-A positive cells in lung sections of these two patients. Strikingly, in patient 1, we observed diffuse and intense expression of SP-A in the pulmonary alveoli suggesting hyperplasia of type II pneumocytes (figure 3A). This was in line with the alveolar epithelial hyperplasia found in H&E staining. Additionally, SP-A expression was also observed in the hyaline membrane (figure 3B). A similar pattern was obtained in patient 2 (figure 3C). Immunostaining of a normal lung section was performed in parallel to exclude the possibility of overcolourisation (figure 3D). To further verify the hyperplasia of type II pneumocytes and to exclude a possible change due to bronchitis in patient 1, we performed additional immunohistochemistry of SP-B in both patients. In support of our observations, a diffused pattern of SP-B staining was also observed in infected lungs (see online supplementary figure 2A–B), whereas, normal lung had punctate signal (see online supplementary figure 2C). Furthermore,

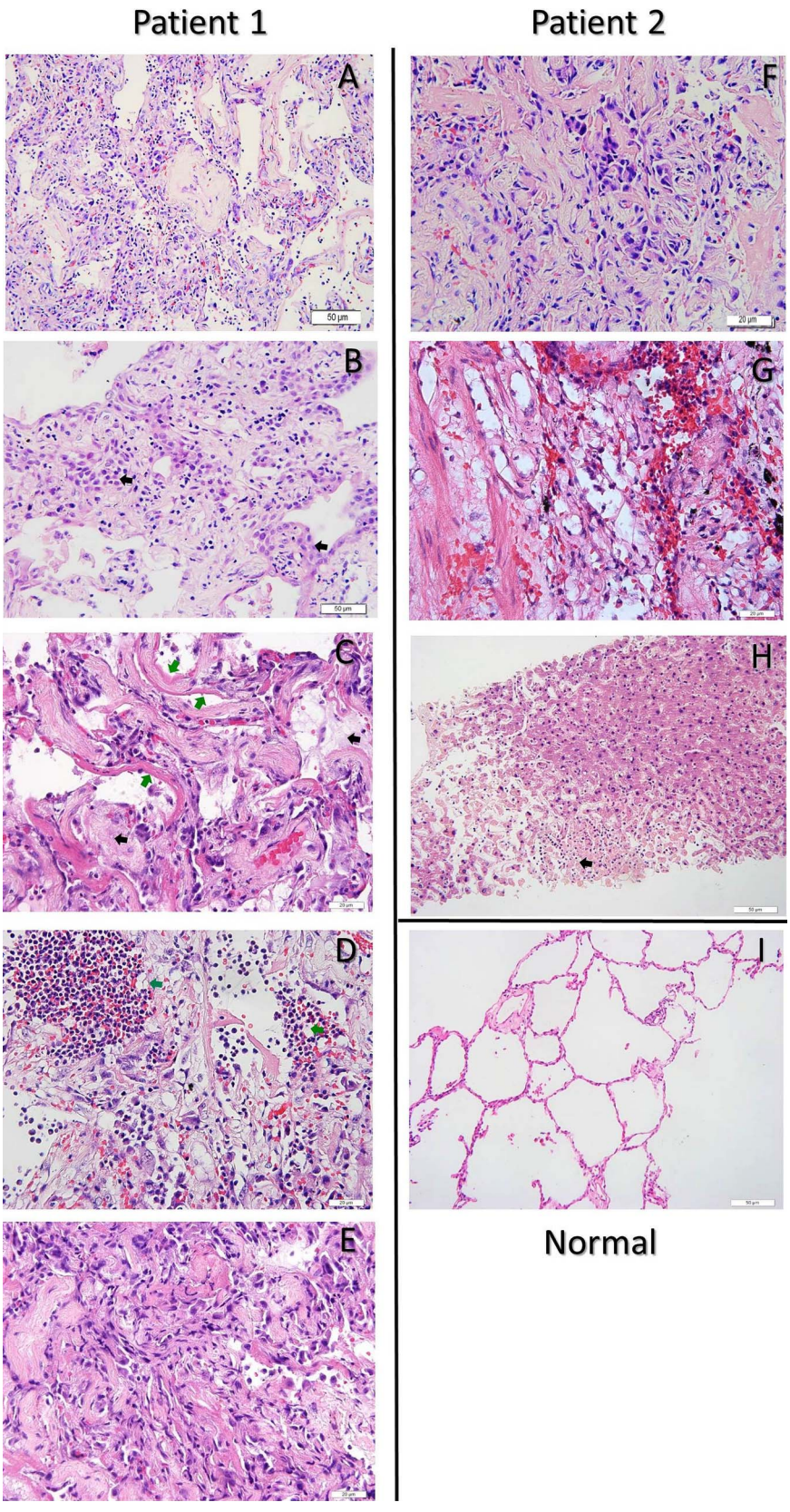

Figure 1 Histopathological findings in the lung and liver tissues from two fatal H7N9 influenza infections. (A) Diffuse alveolus injury, widened alveolar septum, inflammatory cells and serous effusion in the alveolar space, ×200. (B) Phlogocyte infiltration and type II pneumocyte hyperplasia (black arrows), ×400. (C) Serosity exudation (black arrows) and hyaline membrane formation (green arrows), ×400. (D) Neutrophils infiltration in the alveolar space in the alveolar tissue (green arrows), ×400. (E) Exudate organisation, alveolar septum fibrosis and pulmonary consolidation, ×400. (F) Fibroproliferative changes, meshwork of hyaline membrane and pulmonary consolidation, ×400. (G) Intra-alveolar haemorrhage. (H) Hepatic spotty necrosis accompanied by inflammatory cells infiltration and fatty degeneration in some hepatocytes, ×400. (I) Typical H&E staining result of a normal lung, ×200. A–E are from patient 1; F–H are from patient 2.

immunostaining of CD68 generated intense and clustered positive signals indicative of macrophage proliferation (figure 3E) compared with normal control (figure 3F).

Next, we evaluated the distribution of intrapulmonary CD3T lymphocyte and, more specifically, T helper cells (CD4+) and cytotoxic T lymphocytes (CD8+). In patient 1, we found rare infiltration of CD3+ T lymphocytes in the interstitial spaces (figure 4 A). Moreover, virtually no CD4+ cells (figure 4B) but only a few scattered CD8+ cells (figure 4 C) were found in the pulmonary tissues. Immunostaining assays in patient 2 exhibited

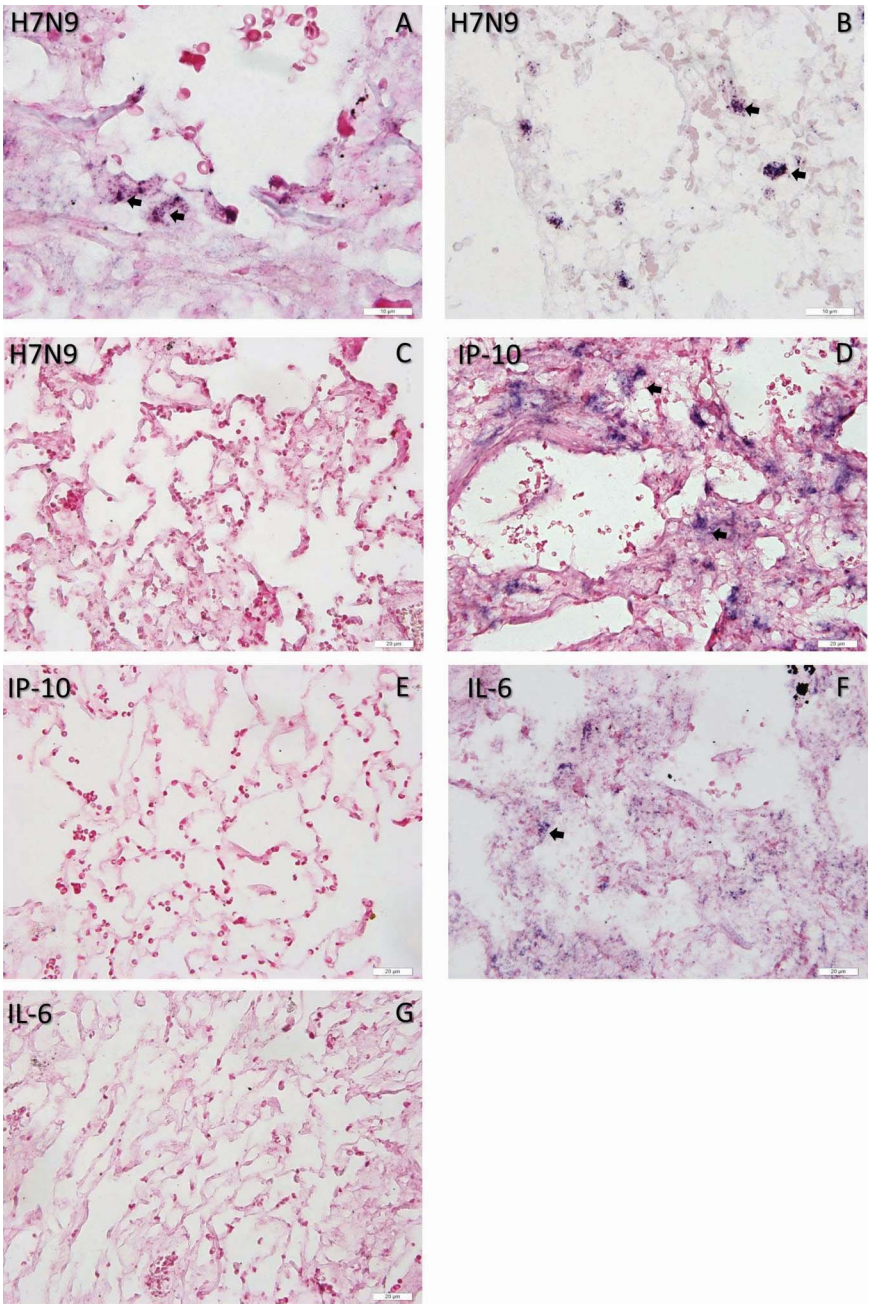

Figure 2 In situ hybridisation of H7N9 RNA and mRNAs of inflammatory mediators. Detection of nucleoprotein mRNA of H7N9 avian influenza virus in patient one (A), in C57BL/6 mice experimentally infected with an H7N9 isolate (B), ×1000, and in normal lung (C), ×400. IP-10 (D) and interleukin-6 (F) mRNAs were detected in lung sections of patient 1, but were absent in normal lung tissue (E, G), ×400.

a similar pattern, although more lymphocytes resided in the pulmonary tissue (see supplementary figure 3A–C). Indeed, the peripheral lymphocyte counts (patient 1, CD3, 127; CD4, 92; CD8, 36; patient 2, CD3, 347; CD4, 278, CD8, 72; normal range, CD3, 690–2540; CD4, 410–1590; CD8, 190–1140; all in 10^6/L) in the late stage of infection in these two patients showed analogous trend. The histological analysis and blood cell count data suggested a general decline of lymphocytes both in peripheral and in H7N9 virus-infected tissue.

Apart from the proposed 'cytokine storm' theory for immunopathology of severe influenza infection. Monsalvo *et al* reported that high titres of low avidity antibody for pdm09H1N1 influenza virus led to immune complex-mediated complement activation.[12] We thus tested whether the formation of immune complex may also have contributed to the pulmonary pathology ensuing H7N9 virus infection. To examine this, we used an antibody against C4d, a sensitive and reliable marker for complement deposition.[13] Since pathogenic fungi have been reported to be potent inducers of complement activation cascade,[14] pulmonary tissue from a patient with Aspergillus infection was tested in parallel as positive control (figure 4G). We found that no measurable C4d signal was obtained from the lungs of patients 1 and 2 (figure 4D, E) similar to normal control (figure 4F). These data suggest that immune complex-mediated pulmonary damage may not participate in H7N9 influenza-induced immune pathology.

DISCUSSION

Human infection of H7N9 avian-origin influenza usually presented with fever and cough at the onset of disease which can further develop into pneumonia and ARDS with high rates of ICU admission and death.[2] After the first wave of the epidemic during March–May 2013, H7N9 influenza virus has re-emerged from the winter of 2013 until now with over 200 new cases.

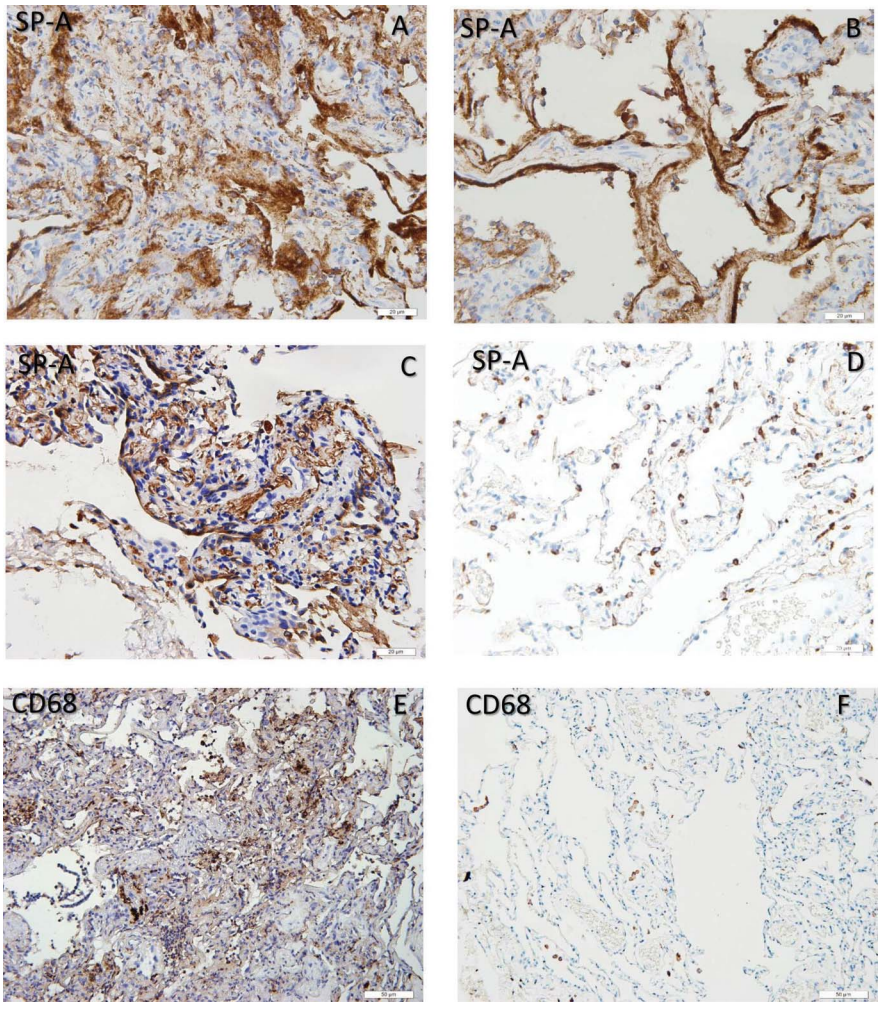

Figure 3 Immunohistochemistry of surfactant protein A (SP-A) and CD68. Expression of SP-A in lung sections from patient 1 (A, B), patient 2 (C), and in normal lung (D), ×400. The expression of CD68 in lung sections from patient 1 (E) and in normal lung (F), ×200.

There has been only one report describing the pathological changes in pulmonary and extrapulmonary tissues following H7N9 influenza infection.[7] The major histological characteristics reported therein, including diffuse alveolar damage, hyaline membrane and fibroproliferation in the lung and spotty necrosis in the liver, are generally in agreement with our results. Additionally, we extended these observations by conducting detailed analyses of some key immunological aspects of H7N9 virus-induced pathogenesis using in situ hybridisation and immunohistochemistry.

We first visualised the site of viral replication using a probe set for targeting NP mRNA. We observed a weak positive signal in lung samples from patient 1. This weak signal was expected because at the time of biopsy, his latest throat swabs had tested negative for H7N9 (qPCR, data not shown). Additionally, the scattered but not diffuse nature of positive cells was in agreement with another study on H5N1-infected patients.[11]

Like H5N1 infection,[15] a prominent clinical feature of H7N9 influenza infection is lymphopenia. Gao *et al*[2] reported that 88.3% of the 111 H7N9 infected individuals presented with low levels of peripheral lymphocytes. However, the status of infiltrated lymphocytes, granulocytes and resident macrophages in the alveoli are largely undefined. The immunostaining analyses of CD3, CD4 and CD8T cells indicated that, similar to what was observed in peripheral blood, pulmonary lymphocytes were also rare. The detection of CD68 positive cells in the lung revealed that macrophages were clustered and activated. Additionally, massive infiltration of neutrophils was found in patient 1. However, this is most likely caused by secondary bacterial infection which is a common complication in fatal influenza virus infection.[8] In summary, histological observations indicated that depleted T lymphocytes, varying number of neutrophils and highly abundant and activated macrophages are characteristic of H7N9 infection in the alveoli. In addition to the estimation of infiltrated and resident immune cells, we further detected high levels of intrapulmonary inflammatory mediators, for example, IP-10 and IL-6. Indeed, hypercytokinaemia in H7N9 influenza-infected individuals and experimentally infected mice has been reported by several groups. Moreover, high levels of circulating IL-6 and IP-10 were highly indicative of severe clinical manifestations.[16–18] Our results suggest that IP-10 is produced in the pulmonary alveoli which serves as chemoattractant for monocytes/macrophages and other lymphocytes. Additionally, IL-6 was also detected in the alveoli which further aggravates inflammatory responses.

Since our histological observations indicated hyperplasia of type II pneumocytes, we further detected the localisation of SP-A-positive cells in pulmonary sections. Strikingly, an intense and diffuse signal was detected throughout the alveoli indicating marked proliferation of type II pneumocytes. Moreover, SP-A was also localised to hyaline membranes and this was further confirmed by immunostaining of SP-B protein. We speculate that necrotic type II pneumocytes upon lysis released SP-A/SP-B proteins into the hyaline membrane. Interestingly, SP-A has been

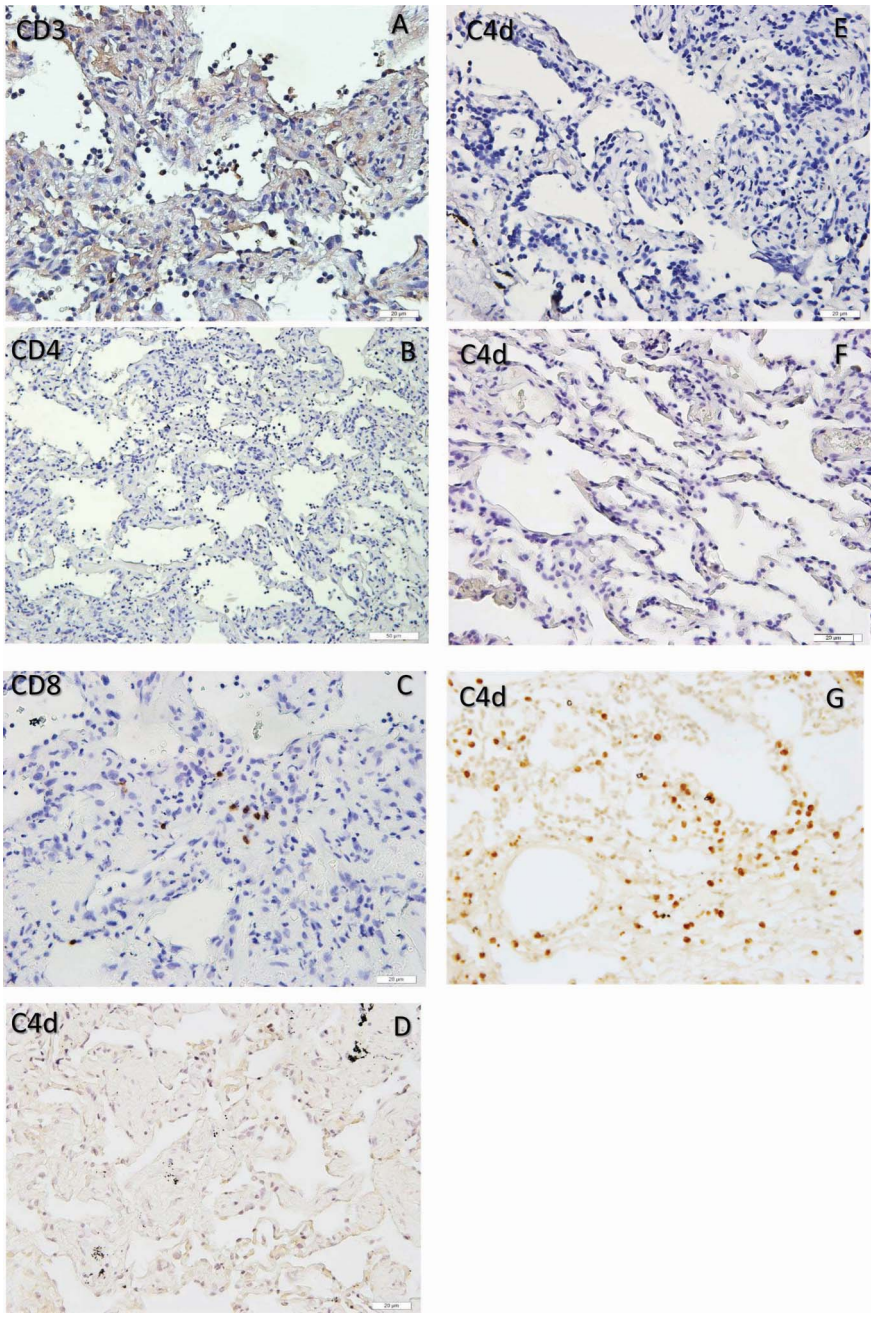

Figure 4 Immunohistochemistry of T lymphocyte infiltration and complement activation. Sporadic CD3+ T cells were detected in the alveolar space (A), ×400. Almost no CD4+ T helper cells were found (B), ×200, whereas, few CD8+ T cells were scattered in the lung tissues in patient 1 (C), ×400. No obvious C4d deposition in H7N9 infected lungs from patient 1 (D) and patient 2 (E) which was similar to that in normal lung (F), ×400. Intense C4d signal was obtained from a patient infected with Aspergillus (G), 400×.

reported to bind to a variety of pathogens including influenza A virus.[19 20] This interaction can further enhance the phagocytosis of macrophages. Indeed, clusters of CD68-positive cells were widespread in parallel with diffused SP-A signals. Thus, we infer that H7N9 infection might cause activation of macrophages via SP-A which, in turn, induces damage and, in some cases, regeneration of type II pneumocytes.

Finally, we tested whether complement-mediated injury took part in H7N9-induced pulmonary pathology. Immunohistochemistry of C4d did not detect obvious complement deposition in pulmonary tissues. The difference between 09pdmH1N1 and H7N9 influenza-induced pathologies seems to stem from the strikingly different serological status against these two viruses in the general population. Virtually, no seropositivity specific for H7N9 virus was present in the Chinese population,[5 21] whereas, low-avidity IgG for H1N1 virus was widespread and associated with severity of disease.[12]

In conclusion, using a combination of routine and molecular pathology methods, a more thorough understanding of H7N9 influenza-induced immune pathogenesis was obtained. The robust proliferation of avian-origin H7N9 influenza virus in the lower respiratory tract caused overt activation of innate immune response, exemplified by production of inflammatory mediators in intrapulmonary macrophages and alveolar cells. This, in turn, resulted in necrosis, but at the same time in regeneration of some type II pneumocytes, marked serosity exudation, hyaline membrane formation and fibroproliferation. On the other hand, the adaptive immune response is restrained as evidenced by depletion of T lymphocytes both in lung and in periphery. No immune complex-mediated pulmonary injury was observed. These findings expand our understanding of the H7N9-associated pathogenesis and may provide clues for clinical intervention aimed at preventing death due to H7N9 infection.

Take home messages

- Depleted T lymphocytes, varying number of neutrophils, hyperplasia of type II pneumocytes, and highly abundant and activated macrophages in the pulmonary alveoli are characteristic of H7N9 influenza infection.
- High levels of intrapulmonary inflammatory mediators in H7N9 infection.
- No obvious complement deposition was found.

Contributors Conceived and designed the study (YF and SL); performed the experiments (YF, LH, YZ and DZ); supplied the materials and methods (QC, AZ); supervised the study, analysed the data and wrote the manuscript (YF, LH, LC, YH and ZZ).

Funding This research was supported by the National Megaprojects of China for Infectious Disease (2012ZX1004211 and 2014ZX10004002-005), National Natural Science Foundation of China (81341004), Ministry of Science and Technology (KJYJ-2013-01-01) and Shanghai Municipal Health and Family Planning Commission (2013QLG002).

Competing interests None.

Patient consent Obtained.

Ethics approval This study was approved by the ethics committee of Shanghai Public Health Clinical Center.

Provenance and peer review Not commissioned; externally peer reviewed.

Data sharing statement Additional unpublished data from this study are available to all academic peers upon request.

REFERENCES

1 Gao R, Cao B, Hu Y, *et al*. Human infection with a novel avian-origin influenza A(H7N9) virus. *N Engl J Med* 2013;368:1888–97.
2 Gao HN, Lu HZ, Cao B, *et al*. Clinical findings in 111 cases of influenza A(H7N9) virus infection. *N Engl J Med* 2013;368:2277–85.
3 Hu Y, Lu S, Song Z, *et al*. Association between adverse clinical outcome in human disease caused by novel influenza A H7N9 virus and sustained viral shedding and emergence of antiviral resistance. *Lancet* 2013;381:2273–9.
4 Wang Q, Zhang Z, Shi Y, *et al*. Emerging H7N9 influenza A (novel reassortant avian-origin) pneumonia: radiologic findings. *Radiology* 2013;268:882–9.
5 Bai T, Zhou J, Shu Y. Serologic study for influenza A(H7N9) among high-risk groups in China. *N Engl J Med* 2013;368:2339–40.
6 Li Q, Zhou L, Zhou M, *et al*. Preliminary report: epidemiology of the avian influenza A(H7N9) outbreak in China. *N Engl J Med* 2013;24:24.
7 Yu L, Wang Z, Chen Y, *et al*. Clinical, virological, and histopathological manifestations of fatal human infections by avian influenza A(H7N9) virus. *Clin Infect Dis* 2013;57:1449–57.
8 Taubenberger JK, Morens DM. The pathology of influenza virus infections. *Annu Rev Pathol* 2008;3:499–522.
9 Uiprasertkul M, Puthavathana P, Sangsiriwut K, *et al*. Influenza A H5N1 replication sites in humans. *Emerg Infect Dis* 2005;11:1036–41.
10 Zhou J, Wang D, Gao R, *et al*. Biological features of novel avian influenza A(H7N9) virus. *Nature* 2013;499:500–3.
11 Gu J, Xie Z, Gao Z, *et al*. H5N1 infection of the respiratory tract and beyond: a molecular pathology study. *Lancet* 2007;370:1137–45.
12 Monsalvo AC, Batalle JP, Lopez MF, *et al*. Severe pandemic 2009 H1N1 influenza disease due to pathogenic immune complexes. *Nat Med* 2011;17:195–9.
13 Stegall MD, Chedid MF, Cornell LD. The role of complement in antibody-mediated rejection in kidney transplantation. *Nat Rev Nephrol* 2012;8:670–8.
14 Kozel TR. Activation of the complement system by pathogenic fungi. *Clin Microbiol Rev* 1996;9:34–46.
15 de Jong MD, Simmons CP, Thanh TT, *et al*. Fatal outcome of human influenza A(H5N1) is associated with high viral load and hypercytokinemia. *Nat Med* 2006;12:1203–7.
16 Wang Z, Zhang A, Wan Y, *et al*. Early hypercytokinemia is associated with interferon-induced transmembrane protein-3 dysfunction and predictive of fatal H7N9 infection. *Proc Natl Acad Sci USA* 2014;111:769–74.
17 Chi Y, Zhu Y, Wen T, *et al*. Cytokine and Chemokine levels in patients infected with the novel avian influenza A(H7N9) virus in China. *J Infect Dis* 2013;208:1962–7.
18 Mok CK, Lee HH, Chan MC, *et al*. Pathogenicity of the novel A/H7N9 influenza virus in mice. *MBio* 2013;4.
19 Khubchandani KR, Snyder JM. Surfactant protein A (SP-A): the alveolus and beyond. *FASEB J* 2001;15:59–69.
20 Benne CA, Kraaijeveld CA, van Strijp JA, *et al*. Interactions of surfactant protein A with influenza A viruses: binding and neutralization. *J Infect Dis* 1995;171:335–41.
21 Yang S, Chen Y, Cui D, *et al*. Avian-origin influenza A(H7N9) infection in influenza A(H7N9)-affected areas of China: a serological study. *J Infect Dis* 2013;209:265–9.